

Cellular Aggregation In Blood Flow

Platelet or neutrophil aggregation in a shear flow of shear rate G was analyzed by accounting for two body collision hydrodynamics and bonding between receptor pairs that have time-dependent stoichiometry. For an apparent forward rate of GPIIb/IIIa crossbridging of activated platelets of $k_f = 1.78 \times 10^{-11} \text{ cm}^2/\text{sec}$, we calculated the overall efficiency (successful collisions divided by total number of collisions predicted by Smoluchowski theory) for activated platelets to be 0.206 at $G=41.9 \text{ s}^{-1}$, 0.05 for $G=335 \text{ s}^{-1}$, and 0.0086 at $G=1920 \text{ s}^{-1}$, values which are in agreement with efficiencies determined experimentally. Activated neutrophils aggregate in a shear field via bonding of L-selectin to PGSL-1 followed by a more stable bonding of LFA-1 to ICAM-3 and Mac-1 to an unknown counter receptor. For β_2 -integrin mediated neutrophil aggregation (characteristic bond strength of $5 \mu\text{dynes}$) in the presence of Fab against L-selectin, an apparent forward rate of $k_f = 1.57 \times 10^{-12} \text{ cm}^2/\text{sec}$ predicted the measured efficiencies of combined LFA-1 and Mac-1 dependent aggregation over shear rates from 100 to 800 s^{-1} . For a selectin bond formation rate constant equal to that of β_2 -integrin, the colloidal stability of unactivated neutrophils was satisfied for a reverse rate of the L-selectin-PGSL bond corresponding to an average bond half life of 10 msec at a characteristic bond strength of $1.0 \mu\text{dyne}$. To predict the measured collision efficiencies of activated neutrophils, metastable aggregates initially bridged by at least one L-selectin-PGSL-1 bond were calculated to rotate from 8 to 50 times at shear rates from 400 to 3000 sec^{-1} , respectively, before obtaining mechanical stability in sheared fluid of either 0.75 or 1.75 centipoise viscosity. Thus, the interaction time for the transition from meta-stable L-selectin bonding to shear-resistant β_2 -integrin bonding was predicted to be about 50 msec, consistent with a direct visualization of the neutrophil collision. With kinetics determined from homoaggregation experiments, Monte Carlo simulations of heteroaggregation of fully activated platelets and neutrophils at 335 sec^{-1} allowed prediction of the size and composition of all aggregates with time. The Monte Carlo simulation demonstrated that neutrophils promote the rate of consumption of platelet singlets in sheared fluid due to the ability of the large diameter neutrophil to sweep through fluid to capture platelets. This increase in platelet aggregation via heteroaggregation with neutrophils was independent of neutrophil tissue factor or Mac-1 effects on coagulation, and occurred despite the initially low neutrophil/platelet ratio.

Keywords: *neutrophil; platelet; integrin; selectin; von Willebrand factor; fibrinogen; hemodynamics*

Comments Theor. Biol.

2000, Vol. 5, No. 6, pp. 413-435

Reprints available directly from the publisher

Photocopying permitted by license only

© 2000 OPA (Overseas Publishers Association) N.V.

Published by license under the Gordon and Breach

Science Publishers imprint.

Printed in Malaysia

INTRODUCTION

During thrombotic and inflammatory states, the flowing suspension of blood cells in plasma can undergo a change of state as activation of enzymatic and cellular processes result in heterotypic cellular aggregation and deposition of cells on the vessel wall. Additionally, the plasma polymerizes to fibrin due to coagulation cascade activation. Understanding these dynamics of human blood requires: (1) characterization of plasma ligands and cellular receptors, (2) development of the mathematics of receptor-ligand mechanics and kinetics, (3) description of the hydrodynamics of cellular collisions in flow, and (4) development of the mathematical models to account for reactive mixtures of aggregates of varying size and composition in a flow field. This review describes the progress to date in integrating these four avenues of investigation towards a theoretical description of thrombosis under flow. Laboratory studies have focused on platelet and neutrophil homotypic aggregation in a linear shear field or in tube flow. Such studies seek to understand the nature of cellular collisions and the probability of sticking as a function of cellular receptor levels and prevailing hemodynamics. Practical applications include the prediction of risk for acute myocardial infarction or stroke, as well as the identification and hemodynamic/pharmacological testing of anticoagulant and anti-adhesive agents.

I. CELLULAR RECEPTORS AND PLASMA LIGANDS

Platelet homoaggregation and adhesion under flow

Injury to the vessel wall with exposure of tissue factor and collagen triggers a complex set of reactions resulting in prothrombin conversion as well as adhesion and activation of platelets. Platelets can be activated by shear stress or by chemical mediators such as ADP, thrombin, thromboxane. The shear stress induced activation of platelets requires shear rates above 3000 s^{-1} . The activation of the platelets involves shape change and release of ADP, as well as activation of glycoprotein IIb/IIIa (GPIIb/IIIa) receptors. The aggregation of platelets is mediated through fibrinogen crossbridging of GPIIb/IIIa and von Willebrand factor (vWF) interactions with GPIb and GPIIb/IIIa. Both fibrinogen and vWF are present in plasma and can be released by platelets during activation. Fibrinogen binds to GPIIb/IIIa receptors (about 50,000 binding

sites/platelet) in a specific, saturable manner ($K_d = 0.1 \mu\text{M}$)^{1,2} via the dodecapeptide sequence $\gamma_{400-411}$ on the D domain of fibrinogen. With ADP-activated platelets, GPIIb/IIIa is fairly well distributed on the cell surface and pseudopods.³ GPIb is present at about 30,000 sites per platelet and binds glycosylated recombinant vWF A1 domain with modest affinity ($K_d \sim 5 \mu\text{M}$).⁴

Studies of platelets adhesion to surface bound fibrinogen under conditions of flow indicate that fibrinogen can support adhesion via the $\gamma_{400-411}$ domain.⁵ The adhesion of platelets to fibrin is not believed to utilize RGD sequences on the α -chain of fibrinogen.⁶ Also, vWF interactions with the GPIb-IX-V complex play an important role in the rapid, but transient tethering of platelets to the damaged vessel wall or to each other, particularly at elevated shear rates. The fibrinogen attachment is seen to be irreversible but less efficient with increasing shear rates. In contrast, vWF mediated attachments are efficient at high shear rates, but become irreversible only gradually.⁷

In aggregation studies, the collision efficiency ϵ is the ratio of successful collisions resulting in aggregation per unit time to the number of total collisions per unit time based on Smoluchowski linear trajectory theory without viscous interactions (See Section III for more details). ADP-induced aggregation of platelets in flow through tubes has been studied by Goldsmith and co-workers.⁸⁻¹² In those studies, the agonist-induced aggregation in tube flow was studied between mean shear rates of 50 to 2000 s^{-1} as a function of gender, ADP concentrations, and fibrinogen levels. They report enhanced aggregation rates in the presence of red blood cells. Red blood cells not only increase the collision frequency because of augmented diffusion, but also enhance platelet aggregation by releasing ADP. Interestingly, RBCs can prolong the mean contact time during collisions in tube flow by about 60 % due to complex multi-particle interactions.¹¹ Similarly, Hellums and co-workers¹³⁻¹⁵ have applied the population balance equation (PBE) along with the Smoluchowski linear trajectory collision theory to quantify the shear induced aggregation and disaggregation kinetics of platelets.

Neutrophil homoaggregation and adhesion under flow

The unactivated neutrophil presents dimeric P-selectin glycoprotein ligand-1 (PSGL-1) ($\sim 10^4/\text{cell}$) and L-selectin ($\sim 10^4-10^5/\text{cell}$) on the tips of

microvilli.^{16,17} PSGL-1, L-selectin, and ICAM-3 are present on resting neutrophils in a state competent for binding. Both L-selectin and ICAM-3 are shed within minutes following neutrophil activation, while PSGL-1 is redistributed and its activity downregulated.¹⁶ Upon activation, Mac-1 and LFA-1 antigenic levels increase dramatically to about 150,000 Mac-1/cell and about 40,000 LFA-1/cell. Only about 10 % of this Mac-1 and LFA-1 is considered to be in a high avidity state.¹⁸

Several studies have defined the receptor mechanisms that support neutrophil homoaggregation¹⁹⁻²¹ LFA-1 (CD11a/CD18) binding to ICAM-3 as well as Mac-1 (CD11b/CD18) binding to an unknown receptor can facilitate integrin-mediated homoaggregation at low shear rates between 100 and 400 s^{-1} . Below 100 s^{-1} , the role of L-selectin-PGSL-1 binding is very minor since no inhibition of aggregation was observed with blocking antibodies against L-selectin at this shear rate.²⁰ Measured collision efficiencies of fMLP-induced neutrophil aggregation supported by integrins (anti-L-selectin present) drop a hundred-fold as the shear rate is increased from 100 s^{-1} to 800 s^{-1} . Above 100 s^{-1} , L-selectin plays an important role in fMLP-stimulated neutrophil homoaggregation. Unexpectedly, the collision efficiency increases to a maximum at $G = 400 s^{-1}$ and then declines,²⁰ consistent with observations of the "selectin hydrodynamic threshold" effect.^{22,23}

Platelet-neutrophil heterotypic aggregation and adhesion in coagulating flow

The rolling and arrest of neutrophils on activated endothelium or spread platelets involves the transition^{24,25} from P-selectin mediated tethering to more stable integrin bonding^{24,25} Neutrophil PSGL-1 can bond with P-selectin on activated endothelium or platelets. Firm adhesion of the transiently tethered neutrophil to other cells is largely controlled by neutrophil Mac-1 (CD11b/18) binding to: endothelial ICAM-1; platelet GPIIb/IIIa bound fibrinogen²⁶ or other unknown platelet receptors;²⁷ and an unknown neutrophil Mac-1 counter receptor. P-selectin mediated capture of neutrophils by platelets is prothrombotic through various possible mechanisms such as potentiated fibrin formation,²⁸ amplified L-selectin-dependent neutrophil deposition,²¹ and/or volumetric contributions due to aggregation biophysics under flow.^{29,30} The interaction of activated platelets with neutrophils mediated by fibrin(ogen) may

also induce neutrophil oxidative burst. Platelet binding to neutrophils via P-selectin enhances neutrophil respiratory burst. Soluble P-selectin does not appear to activate neutrophil signaling or oxidative burst. Also, aggregates of platelets and neutrophils have metabolic interactions involving arachidonic acid exchange.

The strongest evidence to date that leukocytes promote thrombotic processes and fibrin deposition comes from the baboon femoral arteriovenous shunt model²⁸ comprised of a 5 mm diameter dacron shunt with 100 ml/min blood flow. Monoclonal antibody GA6 against P-selectin reduced indium-labelled leukocyte accumulation by 60 % over a 2 hr time course. GA6 Fab2' fragment reduced leukocyte accumulation by 80 % over 2 hr. Anti-P-selectin dramatically reduced fibrin accumulation by 70 %. A marked reduction of fibrin deposition by anti-P-selectin was seen as early as 5 minutes after the initiation of flow. Palabrica, et al.²⁸ also noted that GA6 reduced the content of red blood cells within the thrombi. While elevated expression of tissue factor requires about 20 min, it is possible that neutrophils elevate the production of thrombin at the site of the clot via Mac-1 binding of factor X and the release of proteases such as elastin and clathespin G.^{31,32} The competition between factor X, fibrinogen, and fibrin for Mac-1 as well as the prevailing levels of Cathepsin G under flow conditions remains largely unquantified from a kinetic point of view.

Neutrophil adhesion to preformed endothelial matrix and fibrin under shear flow was studied recently by Kuijper et al.³³ Although neutrophils can adhere to fibrin via Mac1 at shear stresses up to 20 dynes/cm², soluble fibrinogen inhibited the interaction. Fibrin-mediated steric hindrance of neutrophil attachment to TNF- α treated endothelium was noted by Kirchhofer et al.³⁴ Tijburg et al.³⁵ used a calibrated staining assay to measure deposition of peroxidase-labeled fibrin on endothelial cell matrix (containing tissue factor) from heparinized whole blood. They found that fibrinopeptide A generation was not a function of shear rate at 300 or 1300 s⁻¹. Fibrin deposition to the surface was greater at 300 s⁻¹ than at 1300 s⁻¹. Fibrin monomer (fibrinogen des-A) concentration was greater in the perfusion fluid at 1300 s⁻¹. This study is in contrast to a study with nonanticoagulated whole blood perfused over partially denuded rabbit aortas where platelet and fibrin deposition both increased with shear rate up to 1500 s⁻¹.³⁶ The physical hydrodynamics of fibrin deposition and removal under flow are not fully characterized.

II. RECEPTOR-LIGAND MECHANICS AND KINETICS

Due to the two dimensional surface on which they reside, the kinetics of receptor-ligand binding between cells are more complicated than those in solution. The relative motion of colliding cells can enhance the encounter rates of free receptors on opposing surfaces,³⁷ while the concomitant strain on receptor complexes increases their propensity to dissociate. While there are a number of models for the force-dependence of the off-rate, the most frequently used is that of Bell:³⁸

$$k_{\text{off}} = k_{\text{off}}^{\circ} \exp(-\sigma F/nk_{\text{B}}T) \quad (1)$$

Here, k_{off}° is the off-rate in the absence of an applied force, F is the applied force, n is the number of bonds in the contact area, k_{B} is Boltzmann's constant, and T is the temperature. The parameter σ is denoted the reactive compliance, which scales with the length of the binding pocket. The expression follows directly from a thermodynamic analysis of the bonding, assuming that the change in the internal energy of a receptor-ligand complex may be approximated by the first term of its Taylor series, σF . This is a good approximation, in that the length of a complex may change only slightly. Consequently, other models incorporating higher-order terms³⁹ are difficult to distinguish from the Bell model when working with real cells.

A further complication of two-dimensional receptor kinetics is that the applied forces on bonds vary greatly depending on the type of physical interactions of the cells. For example, a doublet in solution will rotate as a function of its local hydrodynamic environment, requiring the receptor complex to bear twisting forces as well as normal and tangential forces that oscillate in time. Moreover, leukocytes rolling can involve microvilli tether stretching to average lengths of $\sim 5\mu\text{m}$ (D. Schmidtke, submitted), thus shielding the bond from force.⁴⁰ The shared surface area of a pair of cells or aggregates varies greatly on their respective morphologies or means of interaction. In these cases, Bell's model may be inadequate in describing the force dependence of the off-rate over the entire force regime.

Stochastic Formulation

In the contact area between a pair of cells, the number of receptors and ligands is inevitably small. Consequently, the kinetics of adhesion are

best described by a stochastic formalism, which allows for integer populations of biochemical species and their variation. An excellent review of the stochastic approach has been written by McQuarrie.⁴¹ For receptors and ligands populations, r and l respectively, the probability of there being exactly c complexes is:

$$\begin{aligned} dp_c(t)/dt = & Ak_{\text{on}}(r+1)(l+1)p_{c-1}(t) - Ak_{\text{on}}rlp_c(t) \\ & + k_{\text{off}}(c+1)p_{c+1}(t) - k_{\text{off}}cp_c(t) \end{aligned} \quad (2)$$

Here, A is the contact area, k_{on} is the on-rate, and k_{off} the off-rate. This "master equation" has recently been solved exactly (I. Laurenzi, submitted). However, Long et. al.⁴² used an approximate solution to determine the probability of an adhesive event between cells, accounting for the temporal force dependence of the off-rate. For aggregating cells, the sticking probability is then $1-p_0(\tau)$ where τ is the time of contact without receptor-ligand interaction.

Deterministic formulation

Bell⁴³ postulated that for two cells or aggregates brought together by shear flow with collision characterized by characteristic time of collision, τ and collisional contact area, A_{coll} , a successful binding event takes place if:

$$\left\{ \int_0^\tau \frac{dN_b}{dt} dt \right\} A_{\text{coll}} \geq N_{\text{crit}} \quad (3)$$

where dN_b/dt is the net rate of formation of the bonds per unit area formed by reaction of the i - j receptor pair $\{dN_b/dt = 2k_f[N_i][N_j] - k_r[N_b]\}$ and N_{crit} is the critical number of bonds needed to hold the colliding aggregates together. Following Bell,⁴³ the force between the aggregates is estimated to be on the order of the drag force which is assumed to be distributed equally between each of the bonds. The Stokes drag force to break bonds ($F_{\text{drag}} = 6\pi\mu R_{\text{eff}}V_{\text{eff}}$) can be estimated for an effective radius R_{eff} of the projectile sphere in near proximity of the target. Thus, the critical number of bonds are $N_{\text{crit}} = F_{\text{drag}}/f_c$ where f_c is the characteristic force to break a bond. The effective velocity, V_{eff} is the relative velocity between the particles at time of contact. For platelets, fibrinogen is assumed to be in equilibrium with GPIIb/IIIa and the i - j receptor pair is defined as the reaction between free GPIIb/IIIa (~ 500 per platelet) and bound fibrinogen ($\sim 45,000$ /platelet) on the

opposing platelet. The reverse rate of bond dissociation is neglected since the β_3 -integrin bond likely lasts on the order of seconds, significantly longer than the time scale of the collision.⁴⁴

The neutrophil aggregation behavior mediated by integrins (LFA-1 binding ICAM-3 and Mac-1 binding a putative ICAM-3-like receptor) in the absence of L-selectin has been modeled considering that the time dependent level of active LFA-1 and Mac-1 receptors for 1 μM fMLP stimulation of neutrophils at $t = 0$ sec. The 100% maximal activity of LFA-1 and Mac-1 was taken as 10% of the maximal antigenic level (150000 Mac-1/neutrophil; 40,000 LFA-1/neutrophil). The number of ICAM-3 receptors was considered to remain constant at 50,000/neutrophil at the early times before disaggregation begins after about 100 seconds. The rate of bond formation per unit area for integrin mediated aggregation, neglecting bond dissociation during the collision, is given as:⁴⁵

$$\beta_2\text{-integrin bonding} \quad \frac{dN_b}{dt} = 2 k_f [N_{\text{LFA1}}(t)] [N_{\text{ICAM3}}(t)] + 2 k_f [N_{\text{Mac1}}(t)] [N_{\text{ICAM3}}] \quad (4)$$

Neutrophil aggregation mediated by L-selectin binding with PGSL-1 in conjunction with integrins has been modeled considering 50,000 L-selectin and 10,000 PGSL-1 dimer receptors per neutrophil. The rate of formation of selectin bonds per unit area is given as:

$$\text{L-selectin bonding} \quad \frac{dN_b}{dt} = 2 k_f^{\text{sel}} [N_{\text{Lsel}}] [N_{\text{PGSL1}}] - k_r^{\text{sel}} [N_b^{\text{sel}}] \quad (5)$$

For the case of binding through multiple receptors, the total drag force is distributed among the bonds which requires the calculation of the critical number of bonds needed to hold the colliding aggregates by selectin and integrins. As an approximation, two aggregates brought together by the shearing flow are held together if:

$$\frac{\int_0^\tau A_{\text{coll}} \frac{dN_b^{\text{intg}}}{dt} dt}{N_{\text{crit}}^{\text{intg}}} + \frac{\int_0^\tau A_{\text{coll}} \frac{dN_b^{\text{sel}}}{dt} dt}{N_{\text{crit}}^{\text{sel}}} \geq 1 \quad (6)$$

However, if the above deterministic criterion is not strictly satisfied during the duration, τ of the primary collision, any doublet with at least a single L-selectin-PSGL-1 bond is allowed to rotate as a metastable aggregate under the action of the shear flow, due to the stochastic nature of the bond under loading. The rotation of the aggregates provides extra interaction time T_i for bonding to hold the colliding particles together,

i.e., integrals on the LHS of Eq. 6 are carried over longer interaction times T_i beyond the duration τ of the primary collision.

III. HYDRODYNAMICS OF CELLULAR COLLISIONS

Theoretical Analysis

A cell in a slow velocity streamline near the wall acts as a target (or test) particle for a faster moving particle that resides in higher velocity streamlines just slightly further away from the wall than the test particle. The fluid mechanical event of the two-body collision can be realized very precisely in a cone-and-plate viscometer where the shear rate is uniform in the entire fluid volume (i.e. a linear shear field) and the suspension has a cell volume fraction of $\sim 1\%$, thus eliminating multi-body interactions.

The mathematics are well established for collisions of two smooth hard spheres at a shear rate G with interactions of electrostatic interaction and van der Waals attraction in linear shear flow.⁴⁶⁻⁴⁸ The key physical aspect of this interaction is that a significant lubrication effect exists where the squeezing of the viscous fluid from the gap between the cells can often prevent the surfaces from coming in contact. This hydrodynamic interaction causes the cells to follow curvilinear trajectories instead of the linear trajectories employed in Smoluchowski collision theory. The surface roughness of real cells or multicellular aggregates, however, may enhance the drainage of fluid between the cell surfaces and facilitate the close proximity contact between cells and help increase the capture radius of the target cell. For neutrophils, this roughness is estimated to be 400 nm (average length of the neutrophil microvilli) and defines how close the two objects must approach in order for contact to occur (i.e. the capture trajectory).⁴⁵ This distance is more difficult to estimate for platelets since platelets are smooth except for a few prominent pseudopods. Tandon and Diamond⁴⁴ used a distance of 40 nm, the close proximity of the membranes, for platelets to define the capture trajectory.

The van der Waals attraction (Hamaker constant = 10^{-19} J) and electrostatic repulsion ($\psi_0 = -15$ mV) have little effect on the neutrophil hydrodynamics since the neutrophils are so rough, but may have more of a role in platelet collisions. Solution of the governing equations of

motion that describe the two body collision of spheres (**Fig. 1A**) is used to carry out trajectory calculations. Only particles flowing through the cross section defined by the hydrodynamic cross-section in **Fig. 1B** are capable of colliding with the target particle. The flux through this upstream area is used to calculate the collision frequency. However, not all collisions result in successful binding of the colliding aggregates. Only those collision that provide sufficient collision time to form enough receptor mediated bonds to hold the colliding particles together can result in successful aggregation.

Tha and Goldsmith⁴⁹ calculated the forces (shear and normal) for two spheres singlets acting as a doublet:

$$F_{\text{shear}} = \alpha_{yz} \mu G a_1^2 [(\cos 2\theta_y \cos \phi_y)^2 + (\cos \theta_y \sin \phi_y)^2]^{1/2}$$

$$F_{\text{normal}} = \alpha_x \mu G a_1^2 \sin^2 \theta_z \sin 2\phi_z \quad (7)$$

where α_{yz} and α_x are reported by Tha and Goldsmith⁴⁹ and θ_i and ϕ_i are the azimuthal and radial angles with respect to the i th axis.

Analysis of Experimental Aggregation

Platelet Homoaggregation

The forward rate of binding between free GPIIb/IIIa and bound fibrinogen characterizes the average and apparent rate of bond formation. For maximally activated platelets ($N_{\text{rec}}=50,000/\text{platelet}$) and half maximally activated platelets ($N_{\text{rec}}=25,000/\text{platelet}$), the overall efficiency $\epsilon_{\tau+h}$ was calculated for $k_f = 1.78 \times 10^{-11} \text{ cm}^2/\text{sec}$ (**Fig. 2**) for $G = 41.9, 335, \text{ and } 1920 \text{ s}^{-1}$. Good agreement was obtained using $k_f = 1.78 \times 10^{-11} \text{ cm}^2/\text{sec}$ with the values determined from initial platelet singlet consumption rates in flow of platelet rich plasma (PRP) through a tube.^{8,9} The single parameter of k_f provided a suitable prediction of platelet aggregation mediated by fibrinogen for shear rates between 50 and 2000 s^{-1} and modest to high degrees of ADP stimulation. The rate constant k_f can also be estimated from the diffusion limit rate of association of receptors in two dimensions as $k_f = \eta [2\pi(D_i + D_j)]$ where η is the effectiveness factor (actual rate/diffusion limited rate) and D_i and D_j are the diffusion constant of receptors on the opposing membranes. Bell's original estimate⁴³ of $\eta = 0.1$ likely represents an upper limit given the orientational, steric, and membrane constraints limiting bond formation. Ideally, η captures the apparent and average behavior of bond formation

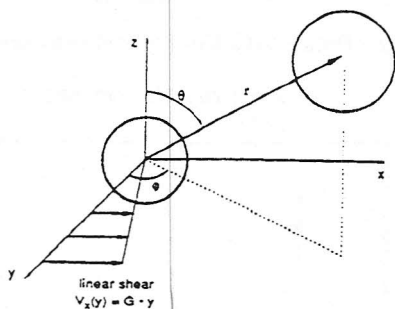
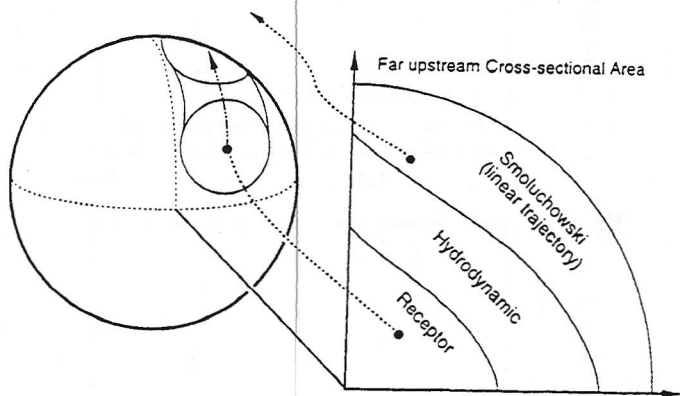
A**B**

FIGURE 1 The two-body collision. Schematic of two, unequal sized spherical cells or their aggregates (of radius a_1 and a_2) in a spherical coordinate (r, θ, ϕ) system (A). The interaction of the particles is investigated in a linear shear field given by $V_x = Gy$ where G is the local shear rate of flow. Schematic of different far upstream cross-section in (B). The *Smoluchowski* upstream area is calculated considering neutrophils follow linear trajectories, while the hydrodynamic collision area is determined from detailed hydrodynamics interactions between colliding aggregates. Whereas the particle flux through the *hydrodynamic* cross-section represents the collision rate between aggregates of radii a_1 and a_2 , the fraction of these collisions that is successful is represented by the flux through the upstream cross-section area labeled *receptor*

between real (rough) platelets, but is not a strong function of particle hydrodynamics. For platelets, $\eta = 0.0178$, indicating that rate of association between free GPIIb/IIIa and bound fibrinogen (-0.19 bonds/ μm^2 per msec) is kinetically controlled in the contact area.

Platelet Aggregation

$$\beta_3\text{-Integrin Rate} = 2(k_f) [\text{GPIIb/IIIa-fibrinogen}] \cdot [\text{GPIIb/IIIa}]$$

$$k_f = 1.78 \times 10^{-11} \text{ cm}^2/\text{sec}$$

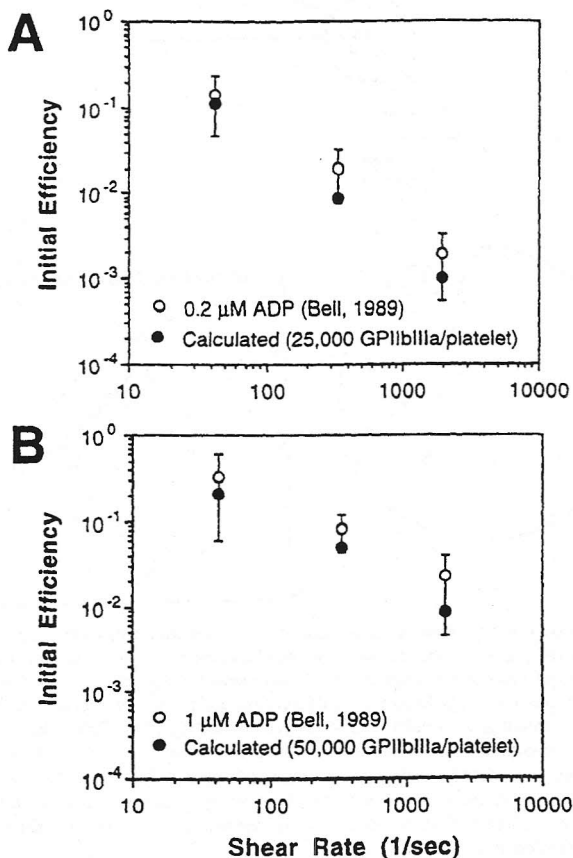


FIGURE 2 Platelet homotypic aggregation. Calculated initial collision efficiencies (ϵ_{r+h}) at $t = 0$ for a forward rate of bonding are compared with measured efficiencies for platelet aggregation at various average shear rates G in tube flow and times in PRP (300,000/ μl and 37 C) with 0.2 μM or 1 μM ADP stimulation. In the model for 0.2 μM ADP stimulation, the receptor level was set half-maximally to 25,000/platelet (A) while for 1.0 μM ADP stimulation, the maximal level of GP IIb/IIIa receptors was set at 50,000/platelet (B). Data from Table II and III of Bell.^{8,9}

Neutrophil Homoaggregation

The instantaneous efficiency for β_2 -integrin mediated neutrophil aggregation in the absence of L-selectin at low shear rates between 100 and 800 s^{-1} is a function of time because of upregulation of Mac-1 and LFA receptors after activation. A time averaged efficiency can be measured experimentally, while instantaneous values of the efficiency can be calculated and then time averaged. For calculating these efficiencies, a single value for the β_2 -integrin forward rate of $k_f = 1.57 \times 10^{-12} \text{ cm}^2/\text{sec}$ was used over the range of shear rates such that the predicted time-averaged overall efficiencies were in agreement with the observed efficiencies of neutrophil aggregation²⁰ (Fig. 3A). Interestingly, this forward rate constant is in agreement with the estimate of $10^{-12} \text{ cm}^2/\text{sec}$ of Shao and Hochmuth⁵⁰ for neutrophil CD18 binding to an antiCD18 coated bead controlled by micromanipulation. Consistent with the role of primary collisions as the dominant interaction mechanism for integrin mediated aggregation, $k_f = 1.57 \times 10^{-12} \text{ cm}^2/\text{sec}$ ($\eta_{\text{intg}} = 0.00125$) predicted the nearly hundred-fold decrease in the measured, time-averaged collision efficiency as the shear rate increased from $G = 100$ to $G = 800 \text{ s}^{-1}$ (Fig. 3A).

For estimating the parameters ($k_f^{\text{sel}}, k_r^{\text{sel}}, f_c$) to model L-selectin-PSGL-1 binding, Tandon and Diamond⁴⁵ calculated the overall efficiency, ϵ_{r+h} , for singlet-singlet interaction mediated by L-selectin alone at $G = 100 \text{ s}^{-1}$. It is known that L-selectin does not mediate appreciable aggregation by itself. For the half life of L-selectin-PSGL-1 of 10 msec and K_f^{sel} equal to β_2 - k_f , a value of f_c^{sel} of 1 μdyne (10 pN) resulted in essentially no aggregation ($\epsilon < 0.001$), consistent with experimental observations of colloidal stability of resting isolated neutrophils. We have used these values to model selectin mediated neutrophil aggregation. The half life of the L-Selectin-PSGL-1 bond has been recently reported to be about 10–15 msec.⁵¹ Shao and Hochmuth⁵⁰ reported that neutrophil L-selectin and CD18 bind to anti-L-selectin and anti-CD18 on beads, respectively, at similar on-rates. At values of $k_f^{\text{sel}} = 1.57 \times 10^{-12} \text{ cm}^2/\text{sec}$ and $f_c^{\text{sel}} = 1 \mu\text{dynes}$ (10 pN), half lives for the L-selectin-PSGL-1 bond of 100 msec and 1000 msec were calculated to result in appreciable aggregation of resting neutrophils.

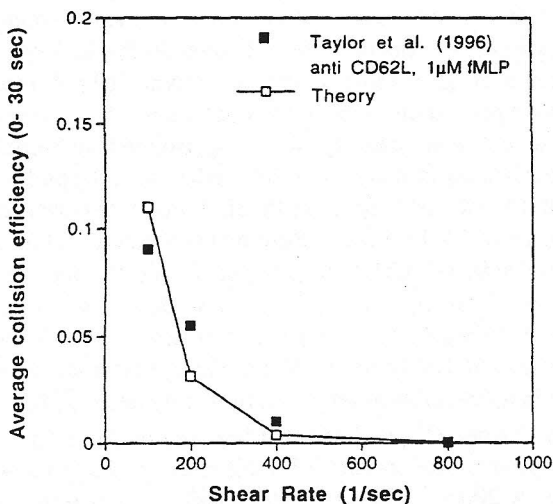
Tandon and Diamond⁴⁵ predicted that bonding during primary collisions were responsible for creation of stable neutrophil aggregates at low shear rates below 200 s^{-1} . However, above 400 s^{-1} , it was necessary to consider additional time needed for integrin bonding to achieve aggre-

gate stabilization to resist breakup. The time-averaged overall collision efficiency ϵ_{r+h} for shear rates between 100 and 3000 s^{-1} (buffer viscosity of 0.75 cP) is shown in **Fig. 3B** for an average interaction time of $T_i = 0$ msec (primary collision only), $T_i = 50$ msec (8 to 50 rotations), and $T_i = \infty$ (all aggregates that have one L-selectin bond after the primary collision). Also, shown in the plot are the corrected collision efficiencies observed in the experiments of Taylor et al.²⁰ While at the lowest shear rates (100 s^{-1} and 200 s^{-1}), the observed efficiencies could be matched by primary collision phenomena that result in shear stable aggregates, longer interaction times requiring doublet rotation were needed to explain the observed efficiencies for shear rates of 400 s^{-1} and above. The number of rotations is calculated to increase from 8 to 50 as the shear rate increases from 400 to 3000 s^{-1} . The calculated interaction time T_i was about 50 msec for shear rates between 400 s^{-1} and 3000 s^{-1} . This interaction time may reflect a characteristic time when L-selectin bonding is essentially at equilibrium or β_2 -integrins stabilize the contact area.

A Neutrophil Aggregation with β_2 -integrins (no L-selectin)

$$\text{Integrin Rate} = 2(k_i) [\text{LFA-1}(t)] \cdot [\text{ICAM-3}] + 2(k_i) [\text{Mac-1}(t)] \cdot [\text{ICAM-3}]$$

$$k_i = 1.57 \times 10^{-12} \text{ cm}^2/\text{sec}$$



B

Neutrophil Aggregation with β_2 -integrins and L-selectin

$$\text{Integrin Rate} = 2 (k_i) [\text{LFA-1}(t)] \cdot [\text{ICAM-3}] + 2 (k_i) [\text{Mac-1}(t)] \cdot [\text{ICAM-3}^*]$$

$$\text{Selectin Rate} = 2 (k_s) [\text{L-selectin}] \cdot [\text{PSGL-1}] - (k_s) [\text{L-selectin-PSGL-1}]$$

$$k_i = 1.57 \times 10^{-12} \text{ cm}^2/\text{sec}, k_s = 69.3 \text{ sec}^{-1}$$

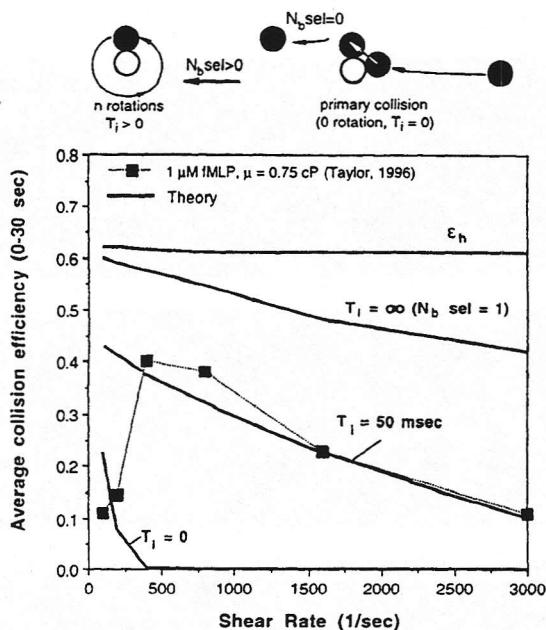


FIGURE 3 Neutrophil homotypic aggregation. The overall collision efficiency, ϵ_{r+h} (averaged over the first 30 sec and the size ratio λ) for integrin mediated aggregation in the absence of L-selectin decreases as a function of shear rate (A). For aggregation mediated simultaneously by β_2 -integrins and L-selectin at a fluid viscosity of 0.75 cP (B), the overall collision efficiency (ϵ_{r+h}) for activated neutrophil as a function of shear rate is shown for: primary collisions ($T_i = 0$, no doublet rotation); after 8 to 50 rotations at shear rates of 400 to 3000 s^{-1} , respectively ($T_i = 50$ msec); and collisions of doublets with at least one L-selectin-PSGL-1 bond at the end of the primary collision ($N_b \text{ sel} = 1$). Also, shown is the maximum possible efficiency if all collisions were successful (ϵ_h), which is the hydrodynamic correction to linear trajectory theory. Shown in (A) and (B) are the experimentally observed collision efficiencies.²⁰

In an effort to investigate the L-selectin-PSGL-1 lifetime during neutrophil collisions, we imaged at 240 frames/sec the collision of a free flowing neutrophil with a surface bound, unspread neutrophil. Although the hydrodynamics are somewhat different than in two body collisions in a shear field, a 38 msec interaction after the primary collision was detected at a wall shear rate of 200 s^{-1} (**Fig. 4**) which is consistent with a predicted 50 msec interaction mediated by L-selectin during neutrophil heteroaggregation.

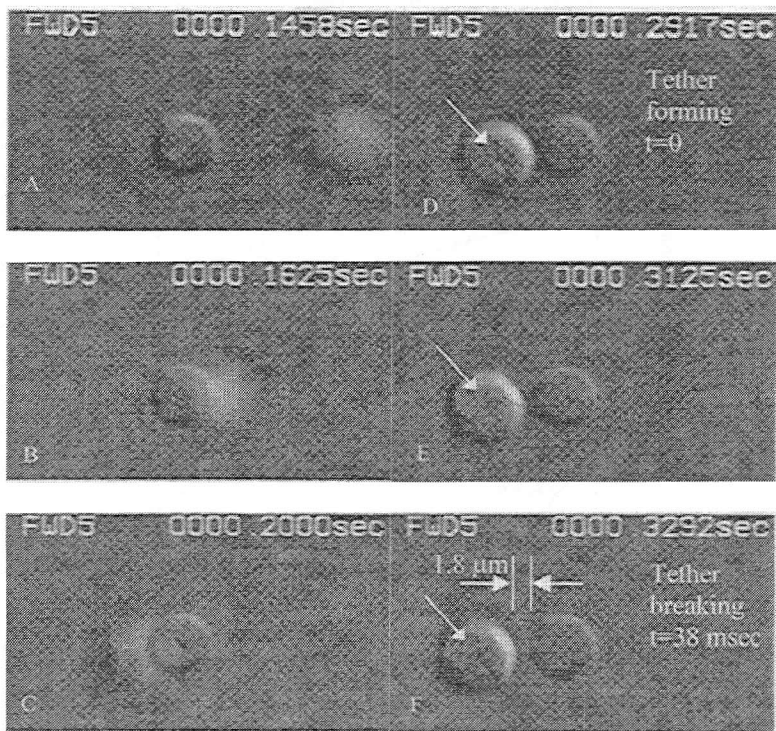


FIGURE 4 Transient L-selectin mediated interactions during the neutrophil-neutrophil collision. High speed imaging (240 frames/sec) at $63 \times$ ($NA = 1.4$) differential interference contrast microscopy of a free flowing neutrophil (frames A and B) being captured (C) and forming a short tether extension before breaking (D-F). The arrows in Frame D-F point to a natural surface feature on the neutrophil which does not rotate, demonstrating that the neutrophil is translating downstream as a microvilli tether(s) grow to a final length of $1.8 \mu\text{m}$ to mediate a 38 msec interaction. The cell is released in the next instant

IV. DYNAMICS OF REACTIVE MIXTURES IN FLOW

Using linear trajectory analysis, Smoluchowski in 1917 defined for the collision frequency for two spheres of volume u and v (or radius a_1 and a_2) undergoing shear-induced aggregation:

$$\beta_G(u, v) = (G/\pi)[u^{1/3} + v^{1/3}] \text{ or } \beta_G = (4G/3)[a_1 + a_2]^3 \quad (8)$$

where G is the shear rate. The collision efficiency ϵ is an empirically determined premultiplier of β_G that fits the aggregation data. The empirically determined efficiency ϵ , either the instantaneous or time-averaged value $\bar{\epsilon}$, includes effects of both shear flow hydrodynamics and neutrophil receptor biology. To delineate the effects of hydrodynamics and receptor binding on the population dynamics, a modified collision kernel is defined as:

$$\beta = \epsilon_{r+h}\beta_G = \epsilon_r\epsilon_h\beta_G \quad (9)$$

where ϵ_h is the hydrodynamic collision efficiency and ϵ_r is the receptor binding efficiency. The product $\epsilon_h\beta_G$ gives the actual collision frequency considering detailed flow fields around the colliding spherical particles, ϵ_r represents the fraction of actual collisions ($\epsilon_h\beta_G$) that results in receptor binding leading to successful aggregation of the colliding particles. The overall collision efficiency ϵ_{r+h} is the ratio of successful collisions relative to the number of collisions estimated by Smoluchowski equation, and can be compared to experimentally determined values. The successful collision kernel, $\beta(u, v)$, is used in a population balance equation (PBE) to predict the evolution of number densities of particles of different sizes. The PBE defines the rate of change of number density, N_i , of neutrophil aggregates comprised of i singlets and is given as:

$$\frac{\partial N_i}{\partial t} = \frac{1}{2} \sum_{j=1}^{i-1} \beta(j, i-j) N_j N_{i-j} - N_i \sum_{j=1}^{\infty} \beta(i, j) N_j \quad (10)$$

where $\beta(i, j)$ is the successful collision frequency between aggregates comprised of i and j singlets, respectively. The first term on the right hand side (RHS) of Eq. 1 represents the birth of particles with i singlets by aggregation of particles having fewer than i singlets (factor of $1/2$ prevents double counting). The second term of the RHS is associated with the death of the particles with i singlets as a result of them aggregating with all other particles to form even larger particles. For homo-

typic aggregation of platelets or neutrophils, Eqn. 10 can usually be solved numerically.

Platelet-neutrophil heteroaggregation. The platelet-neutrophil heterotypic aggregation^{52,53} has relevance to the progression of thrombosis, unstable angina, and acute myocardial infarction, and complications associated with extracorporeal circulation during surgery. For heterotypic aggregation, solution of the population balance equations is not feasible.

A general and highly efficient Monte Carlo algorithm to solve heterotypic aggregation is described in detail in Laurenzi and Diamond³⁰ and is summarized as follows: First, the initial distribution of species (size and composition) in a volume V is given as an initial condition, whereby each species i is defined by its platelet volume P and neutrophil volume N . After all individual reaction probabilities $c(i,j,t) = \beta(i,j,t)/V$ and the total reaction probability $\alpha = \sum c(i,j,t) X_i X_j$ (where X_i is the number of particles of the i^{th} species) are calculated, two random numbers r_1 and r_2 between 0 and 1 are generated. The value of α is the average probability that two arbitrary species will aggregate in V within dt . The time step is then calculated by $\tau = (1/\alpha) \ln(1/r_1)$ and a particular aggregation event "the μ^{th} reaction" is selected by $\sum_1^{\mu-1} (\alpha_{\nu}) \leq r_2 \alpha \leq \sum_1^{\mu} (\alpha_{\nu})$. After each reaction is selected, the species list is adjusted appropriately and the algorithm continues until a prespecified time is reached or all species coalesce at which point $\alpha = 0$.

Monte Carlo simulations of heteroaggregation ($G = 335 \text{ s}^{-1}$) were performed by Laurenzi and Diamond³⁰ at typical concentrations of platelets and neutrophils: $300,000/\mu\text{l}$ and $5,000/\mu\text{L}$, respectively. Maximally activated platelet singlets undergoing homotypic aggregation in plasma levels of fibrinogen at $G = 335 \text{ s}^{-1}$ ($\beta = 0.05$) have a predicted half-life of 8.5 seconds. Similarly, the half-life of fully activated neutrophil singlets ($\beta = 0.31$) undergoing homotypic aggregation at $G = 335 \text{ s}^{-1}$ was 2.0 seconds. In contrast, the kinetic behavior of heterotypic aggregation of fully activated platelets and neutrophils at $G = 335 \text{ s}^{-1}$ yielded dramatic effects: the half-lives of platelets and neutrophils dropped to 2.4 and 0.11 seconds, respectively; a 3.5-fold reduction for platelets and a 18-fold reduction for neutrophils. The size and composition distribution of platelet-neutrophil aggregates is shown in **Fig. 5**. Initially, heterotypic aggregation dominates, where neutrophils combine with only one or two platelets. Due to the abundance of platelets, these aggregates increase their platelet content in the ensuing moments.

Aggregates with more than one neutrophil do not appear until almost all neutrophil singlets are consumed.

Platelet-Neutrophil Heterotypic Aggregation at $G = 335 \text{ s}^{-1}$

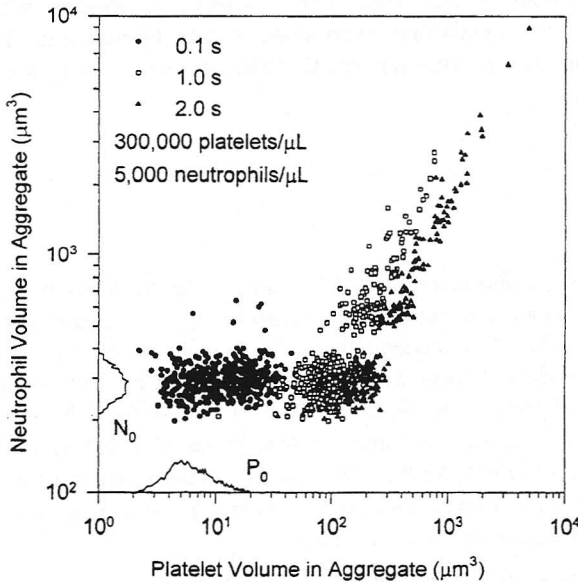


FIGURE 5 Monte Carlo simulation of platelet-neutrophil heteroaggregation. Size and composition distributions are shown for platelet-neutrophil aggregates formed at 335 s^{-1} with full cellular activation. Initial size distributions of the platelets and neutrophil used in the simulation are shown on each axis. For each i and j aggregate containing a platelet volume P and neutrophil volume N , the efficiency $\epsilon_{r+h}(P_i, N_i, P_j, N_j)$ at $G = 335 \text{ s}^{-1}$ was approximated to be a function of the platelet fraction $y_i = P_i/(P_i + N_i)$. Since $\epsilon_{r+h}(y_i, y_j) = \epsilon_{r+h}(y_j, y_i)$, the efficiency was expressed in terms of a single variable, $s = (y_i^2 + y_j^2)^{1/2}$, where $\epsilon_{r+h}(s) = C_1 s^2 + C_2 s + C_3$ where the coefficients fit the experimentally determined values of ϵ_{r+h} for homotypic aggregation of platelets ($s = 2^{1/2}$) and neutrophils ($s = 0$) of 0.05 and 0.31, respectively. The collision of two aggregates containing equal numbers of platelets and neutrophils was considered perfectly sticky ($\epsilon_r = 1$) such that ϵ_{r+h} was approximated as the average hydrodynamic efficiency ϵ_h of 0.61

During co-homotypic aggregation at $G = 335 \text{ s}^{-1}$ platelets and neutrophils after 1.25 seconds, the mean particle volume in co-homotypically aggregating medium is 13 fL, whereas the mean volume for

heterotypically aggregating cells is 357 fL. Moreover, only 2% of the aggregates in a co-homotypic aggregation are larger than 103 fL at 1.25 s, whereas 20% of those aggregating heterotypically fall in this range. Thus, the heterotypic interaction between the two cell types not only promotes generation of more and larger aggregates, but promotes their rate of formation too. Thus, anti-P-Selectin antibodies which are anti-thrombotic agents may exert some of their effects under hemodynamic conditions to alter the kinetics and outcomes of the aggregation biophysics.

SUMMARY

1) The average characteristics of β_3 and β_2 integrin-mediated aggregation of platelets and neutrophils, respectively, in a linear shear field ($G = 50$ to 3000 s^{-1}) is adequately described by the physics of the primary two-body collision with bonding described by a single apparent rate of bond formation ($\beta_3\text{-}k_f = 1.78 \times 10^{-11} \text{ cm}^2/\text{sec}$; $\beta_2\text{-}k_f = 1.57 \times 10^{-12} \text{ cm}^2/\text{sec}$) and a deterministic description of a characteristic bond strength ($f_c \sim 50 \text{ pN}$). As the shear rate is increased, the duration time τ of the primary collision between the colliding particles decreases, and thus the collision efficiency decreases.

2) During neutrophil homotypic aggregation, the description of L-selectin-mediated transient tethering/capture of cells prior to a slower mode of integrin stabilization of the contact area is more complex. Since resting neutrophils that present L-selectin and PSGL-1 do not aggregate in flow, certain limits are dictated for the apparent kinetics and strength of the L-selectin-PSGL bond ($k_f^{\text{sel}} = 1.57 \times 10^{-12} \text{ cm}^2/\text{sec}$, $k_r^{\text{sel}} = 69.3 \text{ s}^{-1}$, $f_c^{\text{sel}} = 10 \text{ pN}$). However, these deterministic parameters fail to describe neutrophil aggregation via contact area stabilization during the primary collision. Analysis of experimental observations support the concept that L-selectin facilitates transient tethering that allows for doublet rotation in the shear field. For the case of neutrophil aggregation in the presence of L-selectin at $G > 400 \text{ s}^{-1}$, metastable aggregates are predicted to rotate for ~ 50 msec under the influence of the flow field providing more time for binding. Evolutionary pressure may select against L-selectin mutations that provide for longer lived L-selectin-PSGL-1 bonds ($t_{1/2} \geq 100 \text{ msec}$) since the aggregation of

resting neutrophils is disadvantageous. The role of vWF in platelet aggregation may be similar to that of selectins.

3) Heterotypic aggregation of platelets and neutrophils can be simulated by Monte Carlo. During heterotypic aggregation in a linear shear field, platelets behaved like an excess reagent in a chemical reaction, used for driving the conversion of another reagent. In this case, the limiting reagent is the neutrophil, which also serves as a catalyst for platelet consumption on account of its large sweep through space. Activated neutrophils serve as nucleation sites for heterotypic aggregation of platelets and other neutrophils.

4) Future efforts need to be directed toward understanding the reaction chemistry and dynamics of heterotypic aggregation between platelets, neutrophils, red blood cells, and fibrin polymer. Also, the effects of aggregate roughness on collisions and deposition are poorly understood. A rigorous formalism of stochastic bond dynamics may be applicable to realistic reaction pathways of multiple bonding pairs in the contact area between real and deformable blood cells. In these approaches, molecular and microscopic aspects of protein stretching, cell deformation, and membrane/microvilli rheology can play a role in controlling the bond life which in turn regulates thrombosis under flow.

Acknowledgements

The authors thank the Southeastern Pennsylvania American Heart Association for support of Drs. Pushkar Tandon and David Schmidtke. This work was supported by a grant from the National Institutes of Health HL-56621. S.L.D. is an established investigator of the National American Heart Association. The authors would like to thank their many colleagues for helpful discussions.

SCOTT L. DIAMOND*, PUSHKAR TANDON,
DAVID SCHMIDTKE and IAN LAURENZI

*Institute for Medicine and Engineering
Department of Chemical Engineering
University of Pennsylvania Philadelphia,
PA 19104*

* Corresponding Author. Tel (215) 898-8652, Fax (215) 573-2093, sld@seas.upenn.edu

References

1. J. S. Bennett and G.J. Vilaire, *Clin. Invest.* **64**, 1393 (1979).
2. G. A. Marguire, T. S. Edgington, and E. F. Plow, *J. Biol. Chem.* **255**, 154 (1980).
3. M. E. Hensler, M. Frojmovic, R. G. Taylor, R. R. Hantgan, and J. C. Lewis, *Am. J. Pathol.* **141**, 707 (1992).
4. M. A. Cruz, R. I. Handin, R. J. Wise, *J. Biol. Chem.* **268**, 21238 (1993).
5. T. N. Zaidi, L. V. McIntire, D. H. Farrell, and P. Thiagarajan, *Blood* **88**, 2967 (1996).
6. R. R. Hantgan, S. C. Enderburg, J. J. Sixma, and P. G. de Groot, *Blood* **86**, 1001 (1995).
7. B. Savage, E. Salvidar, and Z. M. Ruggeri, *Cell* **84**, 289 (1996).
8. D. N. Bell, S. Spain, and H. L. Goldsmith, *Biophys. J.* **56**, 817 (1989).
9. D. N. Bell, S. Spain, and H. L. Goldsmith, *Biophys. J.* **56**, 829 (1989).
10. D. N. Bell, S. Spain, and H. L. Goldsmith, *Thromb. Haem.* **63**, 112 (1990).
11. H. L. Goldsmith, D. N. Bell, S. Braovac, A. Steinberg, and F. McIntosh, *Biophys. J.* **69**, 1584 (1995).
12. H. L. Goldsmith, M. Frojmovic, S. Braovac, F. McIntosh, and T. Wong, *Thromb. Haem.* **71**, 78 (1994).
13. P. Y. Huang and J. D. Hellums, *Biophys. J.* **65**, 334 (1993).
14. P. Y. Huang and J. D. Hellums, *Biophys. J.* **65**, 344 (1993).
15. P. Y. Huang and J. D. Hellums, *Biophys. J.* **65**, 354 (1993).
16. R. E. Bruehl, K. L. Moore, D. E. Lorant, N. Borregaard, G. A. Zimmerman, R. P. McEver, *J. Leukoc. Biol.* **61**, 489 (1997).
17. J. V. Stein, G. Cheng, B. M. Stockton, B. P. Fors, E. C. Butcher, U. H. von Andrian, *J. Exp. Med.* **189**, 37 (1999).
18. M. S. Diamond and T. A. Springer, *J. Cell. Biol.* **120**, 545 (1993).
19. D. A. Guyer, K. L. Moore, E. B. Lynam, C. M. Schammel, S. Rogelj, R. P. McEver, L. A. Sklar, *Blood* **88**, 2415 (1996).
20. A. D. Taylor, S. Neelamegham, J. D. Hellums, C. W. Smith, and S. I. Simon, *Biophys. J.* **71**, 3488 (1996).
21. B. Walchek, K. L. Moore, R. P. McEver, and T. K. Kishimoto, *J. Clin. Invest.* **98**, 1081 (1996).
22. E. B. Finger, K. D. Puri, R. Alon, M. B. Lawrence, U. H. von Andrian, and T. A. Springer, *Nature* **379**, 266 (1996).
23. M. B. Lawrence, G. S. Kansas, E. J. Kunkel, and K. Ley, *J. Cell. Biol.* **136**, 717 (1997).
24. M. B. Lawrence and T. A. Springer, *Cell* **65**, 859 (1991).
25. S. M. Buttrum, R. Hatton, G. B. Nash, *Blood* **82**, 1165 (1993).
26. T. G. Diacovo, S. J. Roth, J. M. Buccola, D. F. Bainton, and T. A. Springer, *Blood* **88**, 146 (1996).
27. V. Evangelista, S. Manarini, S. Rotondo, N. Martelli, R. Polischuk, J. L. McGregor, G. deGaetano, and C. Cerletti, *Blood* **88**, 4183 (1996).
28. T. Palabrica, R. Lobb, B. C. Furie, M. Aronovitz, C. Benjamin, Y. M. Hsu, S. A. Sajer, and B. Furie, *Nature* **359**, 848 (1992).
29. I. A. Hagberg, H. E. Roald, T. Lyberg, *Thromb. Haem.* **80**, 852 (1998).
30. I. Laurenzi and S.L. Diamond, *Biophys. J.* **77**, 1733 (1999).
31. E. Kornecki, Y. H. Ehrlich, D. D. De Mars, R. H. Lenox, *J. Clin. Invest.* **77**, 750 (1986).
32. M. Si-Tahar, D. Pidard, V. Balloy, M. Moniatte, N. Kieffer, A. Van Dorselaer, M. Chignard, *J. Biol. Chem.* **272**, 11636 (1997).

33. P. H. Kuijper, H. I. Gallardo Torres, J. W. Lammers, J. J. Sixma, L. Koenderman, J. J. Zwaginga, *Blood* **89**, 166 (1997).
34. D. Kirchhofer, K. S. Sakariassen, M. Clozel, T. B. Tschoop, P. Hadvary, Y. Nemer-son, and H. R. Baumgartner, *Blood* **81**, 2050 (1993).
35. P. N. Tijburg, M. J. Ijsseldijk, J. J. Sixma, and P. G. de Groot, *Arterioscler. Thromb.* **11**, 211 (1991).
36. K. Ouriel, C. Donayre, C. K. Shortell, C. Cimino, J. Donnelly, D. Oxley, and R. M. Green, *J. Vasc. Surg.* **14**, 757 (1991).
37. K. C. Chang and D. A. Hammer, *Biophys. J.* **76**, 1280 (1999).
38. G. I. Bell, *Science* **200**, 618 (1978).
39. M. Dembo, D. C. Torney, K. Saxman, and D. Hammer, *Proc. Roy. Soc. Lond. B* **234**, 55 (1988).
40. J. Y. Shao, H. P. Ting-Beall, and R. M. Hochmuth, *Proc. Natl. Acad. Sci. USA.* **95**, 6797 (1998).
41. D. A. McQuarrie, *J. Appl. Prob.* **4**, 413 (1967).
42. M. A. Long, H. L. Goldsmith, D. F. J. Tees, and H. L. Goldsmith, *Biophys. J.* **76**, 1112 (1999).
43. G. I. Bell, *Cell Biophys.* **3**, 289 (1981).
44. P. Tandon and S. L. Diamond, *Biophys. J.* **73**, 2819 (1997).
45. P. Tandon and S. L. Diamond, *Biophys. J.* **75**, 3163 (1998).
46. G. K. Batchelor and J. T. Green, *J. Fluid Mech.* **56**, 375 (1972).
47. G. R. Zeichner and W. R. Schowalter, *AIChE J.* **23**, 243 (1977).
48. T. M. Van de Ven, *Colloidal Hydrodynamics*. Academic Press (London) (1989).
49. S. P. Tha and H. L. Goldsmith, *Biophys. J.* **50**, 1109 (1986).
50. J. Y. Shao and R. M. Hochmuth, *Annals Biomed. Eng.* **25**, 200 (1997).
51. M. J. Smith, C. L. Ramos, K. Ley, and M. B. Lawrence, *Annals Biomed. Eng.* **25**, 198 (1997).
52. M. Bcdnar, B. Smith, A. Pinto, and K. M. Mullane, *J. Cardiovasc. Pharmacol.* **7**, 906 (1985).
53. C. S. Rinder, J. L. Bonan, H. M. Rinder, J. Matthew, R. Hines, and B. R. Smith, *Blood* **79**, 1201 (1992).